Magnetic coupling of 4d transition metal monolayers with bcc-Fe as a substrate

1996 J. Phys.: Condens. Matter 8 6607

(http://iopscience.iop.org/0953-8984/8/36/013)

J. Phys.: Condens. Matter **8** (1996) 6607–6616. Printed in the UK

Magnetic coupling of 4d transition metal monolayers with bcc-Fe as a substrate

R Gómez Abal, A M Llois† and M Weissmann

Departamento de Física, Comisión Nacional de Energía Atómica, Avenida del Libertador 8250, 1429 Buenos Aires, Argentina

Received 29 April 1996, in final form 2 July 1996

Abstract. We make a systematic study of 4d transition metal monolayers epitaxially grown on bcc-Fe(001). For this purpose we consider the slabs X/2Fe/X and X/5Fe/X (X = Mo, Tc, Ru, Rh and Pd) within a mean-field Hubbard model. To parametrize the surfaces we add extra orbitals outside the slab to allow for electron spillover. This calculation gives a different polarization for each of the five d orbitals of the transition metals. We find that Mo and Tc couple antiferromagnetically to Fe while Ru, Rh and Pd couple ferromagnetically. Ru presents a more critical behaviour than any other 4d transition metal. The results obtained can be explained through an analysis of bulk paramagnetic d-band centres.

1. Introduction

The development of new sophisticated techniques for producing epitaxially grown metallic structures has led to the derivation of a new set of phenomena such as giant magnetoresistance in ferromagnet/normal metal superlattices and the onset of magnetism in materials that are paramagnetic in the bulk.

Examples of the last case are 4d transition metals, which have been the subject of a great number of contributions reported in the last few years. It has been seen experimentally that a monolayer of Ru epitaxially grown on bcc-Fe in the (001) direction presents an induced spin polarization which corresponds to a magnetic moment of $0.7\mu_B$ per atom [1]. A Pd monolayer on bcc-Fe(001) has also been shown to grow epitaxially and acquire a magnetic ordering [2]. Rh adlayers on bcc-Fe show nonepitaxial growth, but also acquire a magnetic ordering [3]. 4d ferromagnetism was also obtained by epitaxial growth of Ru on a graphite substrate [4].

On the other hand, a lot of theoretical work has also been done on this kind of system, mostly by *ab initio* methods based on the local density approximation of the density functional theory. A Rh monolayer on gold has been shown to be ferromagnetic [5] with a magnetic moment of $1.09\mu_B$ per atom. Also, FLAPW calculations [6, 7] have shown ferromagnetic ordering for Tc ($0.29\mu_B$), Ru ($1.73\mu_B$) and Rh ($1.04\mu_B$) monolayers on Ag(001). No magnetic solution was found for Pd. Very similar results were obtained for 4d transition metal monolayers on Au(001) except in the case of Tc, which shows no magnetic moment [8]. The same method of calculation was used for Ru, Rh and Pd grown

† Also at Departamento de Física, Facultad de Ciencias Exactas y Naturales, Universidad de Buenos Aires, Argentina.

0953-8984/96/366607+10$19.50

on bcc-Fe(001); all of them showed a ferromagnetic ordering with $\mu_{Ru} = 0.49\mu_B$ [3], $\mu_{Rh} = 0.82\mu_B$ [3] and $\mu_{Pd} = 0.29\mu_B$ [2].

To get a better insight into the physics underlying the 4d magnetism in low-dimensional systems, we perform a systematic study of the electronic and magnetic properties of 4d transition metal monolayers on bcc-Fe(001). For this purpose we use a tight-binding Hubbard Hamiltonian in the unrestricted Hartree–Fock approximation. With this model we can analyse the contribution of the different d orbitals to the magnetic moment and its possible relation to magnetic anisotropy. We show that the magnetic coupling information is essentially contained in the tight-binding parameters of the bulk paramagnetic materials.

We study the slabs X/2Fe/X and X/5Fe/X (X = Mo, Tc, Ru, Rh and Pd). For the growth structure a bct lattice is considered, such that the overlayer matches Fe but the cell volume corresponds to the density of the 4d transition metal bulk. This gives a c/a ratio ranging from 1.15 to 1.2.

2. Method of calculation

For the calculations we use a tight-binding Hamiltonian with the parameters of the bulk materials. The magnetism is obtained from a Hubbard-like term solved in the unrestricted Hartree–Fock approximation. This method has been used previously for 3d transition metal slabs and superlattices [9, 10, 11] and the results compare well with *ab initio* calculations.

All many-body contributions appear in the Hartree–Fock approximation in the diagonal term $\varepsilon_{im\sigma}$ given by

$$\varepsilon_{im\sigma} = \varepsilon^0_{im} + \sum_{m'} U_{imm'}\,\Delta n_{im'} + (-1)^{\sigma} \sum_{m'} \frac{J_{imm'}}{2}\mu_{im'} \tag{1}$$

where $\Delta n_{im'}$ is the electronic occupation difference per layer and per orbital with respect to the bulk paramagnetic values, and $\mu_{im'}$ is the magnetization, also per layer and per orbital.

The single-site (ε^0) and hopping elements of the Hamiltonian are obtained for the bulk pure materials from Andersen's canonical LMTO-ASA bands (see [12]). In a crystal with cubic symmetry the diagonal elements for the d bands split into two sets, e_g and t_{2g}, but in the overlayer there is no such symmetry and these values are averaged in the calculations. The dependence of these parameters on interatomic distance and volume per atom was obtained using reference [13] and also by recalculating for the pure paramagnetic materials with the LMTO-TB method. No significant differences were found using the two sets of parameters.

$U_{imm'}$ are the screened intrasite Coulomb integrals in the solid, and their effect is to avoid the large charge transfers which appear in nonselfconsistent tight-binding calculations. Their values were taken from [14]. $J_{imm'}$ are the intrasite exchange integrals and are assumed to be zero except for for d orbitals. For Fe, J_{dd} is fitted performing a calculation for bcc-Fe so as to give the bulk magnetization. We obtained $J_{dd} = 1.05$ eV. The J_{dd}-values for the 4d transition metals were taken from LMTO calculations [12].

The added extra orbitals outside the slabs were chosen as in [9] where we proved that the results do not depend critically on the corresponding parameters.

This Hubbard model also offers the possibility of performing selfconsistency in each d orbital instead of doing it on average, and this may help in the understanding of the details of the magnetic coupling of the Fe and the 4d transition metal. To do this we must go back to the original many-body Hamiltonian in the Hartree–Fock approximation. For simplicity we shall suppose now that the indices m, m' in equation (1) run only over the five d orbitals

and drop the lattice index i. Therefore, for average selfconsistency,

$$\varepsilon_{d\sigma} = \varepsilon_d^0 + U_{dd}\,\Delta n_d + (-1)^\sigma \frac{J_{dd}}{2}\mu_d. \tag{2}$$

This equation comes from the more general one

$$\varepsilon_{m\sigma} = \varepsilon_m^0 + \sum_{m'} \widetilde{U}_{mm'}\langle c^\dagger_{m'-\sigma} c_{m'-\sigma}\rangle + \sum_{m'\neq m} (\widetilde{U}_{mm'} - \widetilde{J}_{mm'})\langle c^\dagger_{m'\sigma} c_{m'\sigma}\rangle \tag{3}$$

if all $\tilde{U}_{mm'}$ and $\tilde{J}_{mm'}$ are assumed to be equal ($\widetilde{U}_{dd}$ and $\widetilde{J}_{dd}$) and $\langle c^\dagger_{m\sigma} c_{m\sigma}\rangle = (n_m + (-1)^\sigma \mu_m)/2$ to be independent of orbital m. U_{dd} and J_{dd} from equation (2) become then linear combinations of $\widetilde{U}_{dd}$ and $\widetilde{J}_{dd}$. Removing the last assumption one can obtain selfconsistency for each orbital separately using the same two parameters, $\widetilde{U}_{dd}$ and $\widetilde{J}_{dd}$, for the screened Coulomb and exchange integrals in equation (3). Effective $U_{dd'}$s and $J_{dd'}$s are then obtained for each different d orbital.

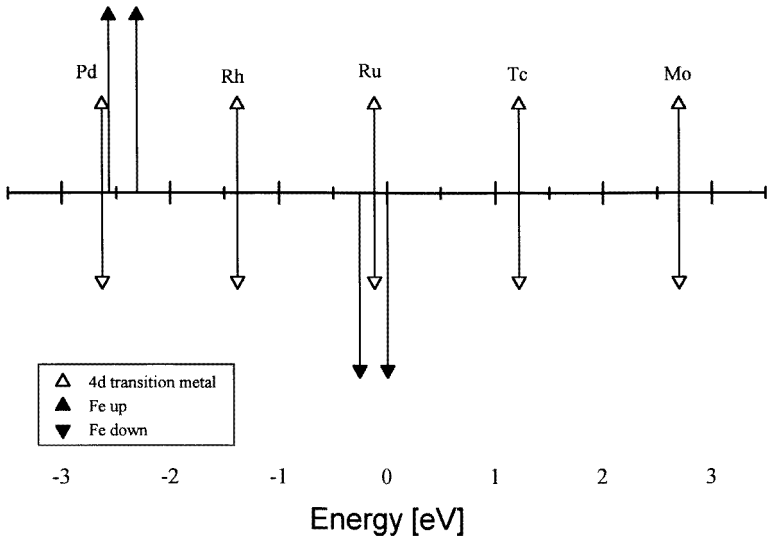

Figure 1. Paramagnetic site energies of the 4d transition metals compared to the ferromagnetic site energies of Fe. The site energy of the higher Fe band was taken as zero.

Table 1. Magnetizations (μ_B) per atom for X/2Fe/X slabs (X = Mo, Tc, Ru, Rh, Pd) obtained by performing selfconsistency on average and on each d orbital separately.

	X	Mo	Tc	Ru	Rh	Pd
Average	μ_X	−0.10	−0.33	0.30	0.76	0.25
selfconsistency	μ_{Fe}	1.85	1.91	2.21	2.62	2.88
Selfconsistency	μ_X	−0.06	−0.20	0.68	0.77	0.17
on each d orbital	μ_{Fe}	1.80	1.92	2.08	2.50	2.70

The Hamiltonian is solved selfconsistently, obtaining the electronic occupation for each layer, orbital and spin. The calculations are performed in the two-dimensional irreducible zone using 256 special k-points from [15].

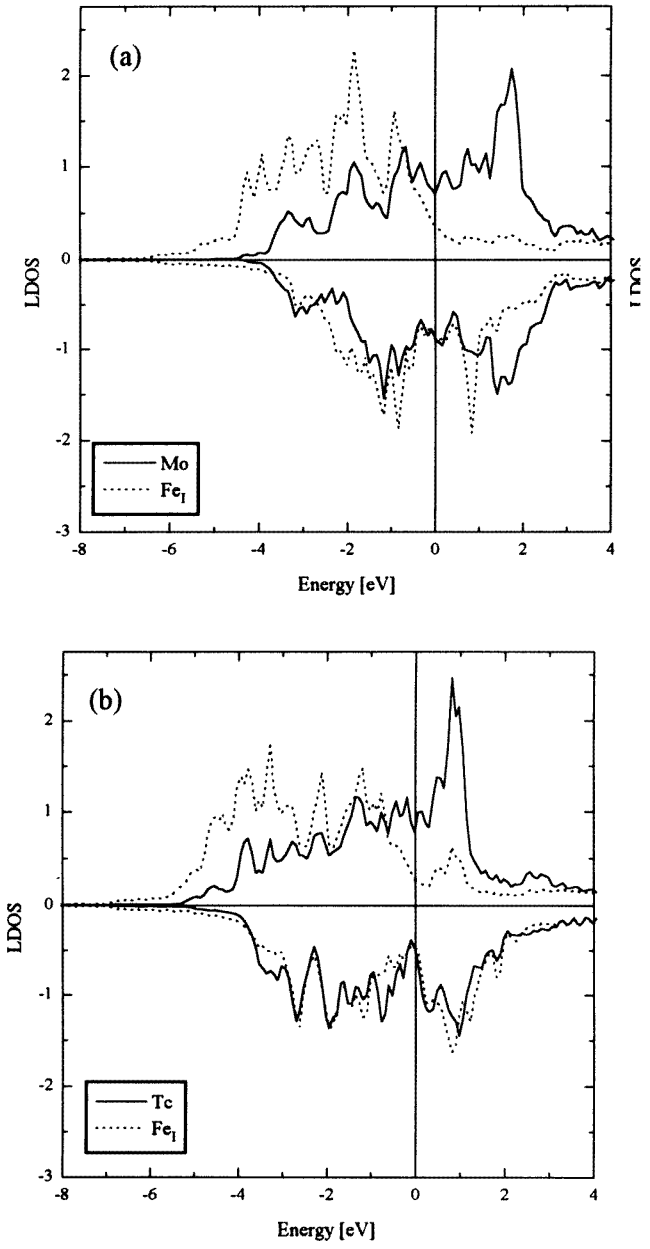

Figure 2. Local densities of states in X/5Fe/X slabs (X = (a) Mo, (b) Tc, (c) Ru, (d) Rh, (e) Pd). The dotted line is the interfacial Fe LDOS. The Fermi energy is taken as zero.

3. Results and discussion

In table 1 we show the magnetic moment per atom for the X/2Fe/X slabs when selfconsistency is performed on each d orbital separately and on average. Table 2 contains the same results for the X/5Fe/X slabs. In all of them the same trends can be observed.

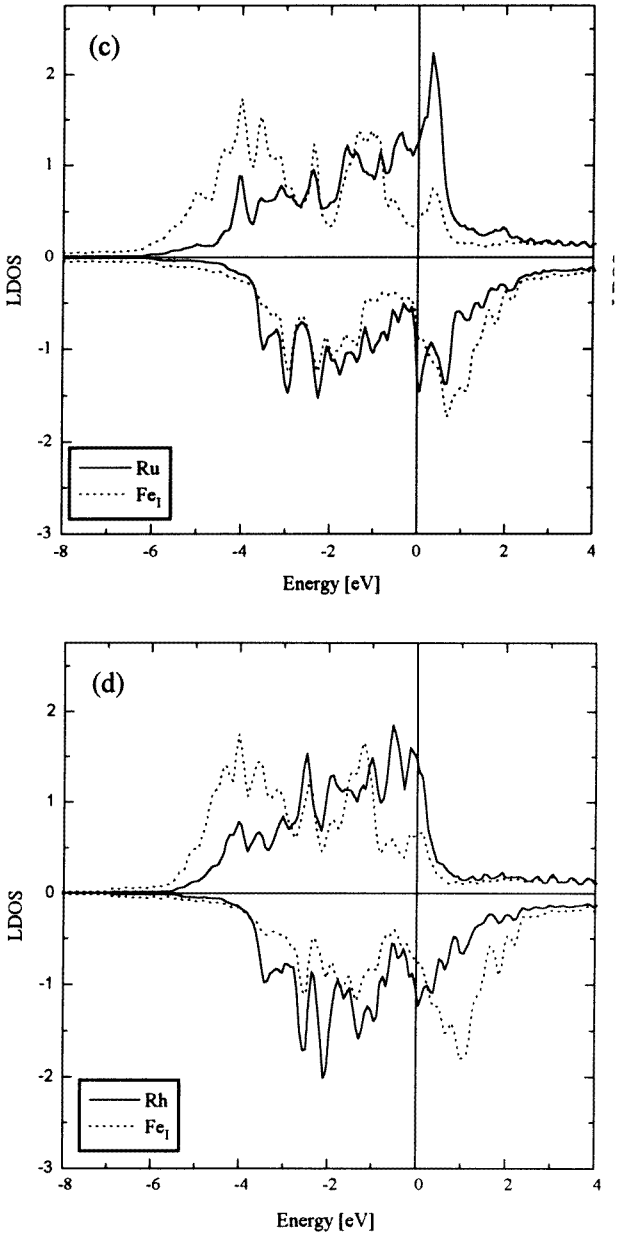

Figure 2. (Continued)

The early 4d transition metals (Mo and Tc) couple antiferromagnetically to iron while Ru, Rh and Pd acquire a ferromagnetic coupling, Rh being the one which presents the largest polarization. In the following paragraph a simple explanation of these different magnetic couplings is given by looking at the relative position of the paramagnetic site energies of the 4d transition metal and the ferromagnetic site energies of Fe obtained from a calculation for bulk bcc-Fe.

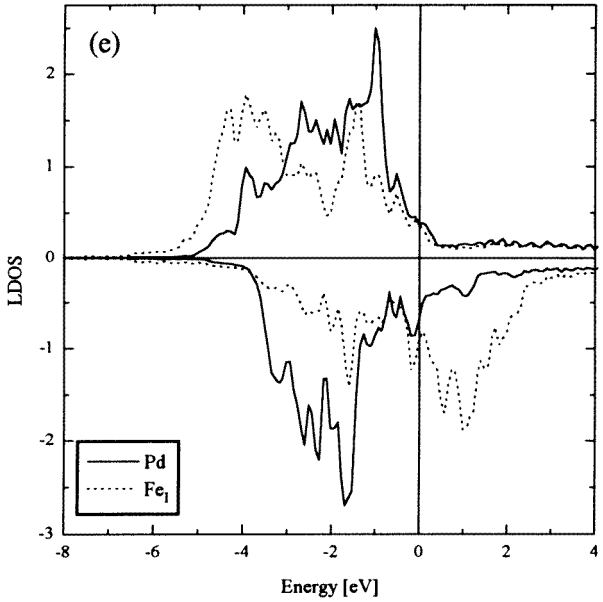

Figure 2. (Continued)

Table 2. Magnetizations (μ_B) per atom for X/5Fe/X slabs (X = Mo, Tc, Ru, Rh, Pd) obtained by performing selfconsistency on average and on each d orbital separately. The subscript I (C) stands for interface (centre).

	X	Mo	Tc	Ru	Rh	Pd
Average selfconsistency	μ_X	−0.23	−0.21	0.06	0.53	0.23
	μ_{Fe_I}	1.50	1.68	1.89	2.25	2.69
	$\mu_{Fe_{I-1}}$	2.32	2.41	2.35	2.26	2.18
	μ_{Fe_C}	2.16	2.22	2.18	2.13	2.08
Selfconsistency on each d orbital	μ_X	−0.14	−0.11	0.42	0.83	0.15
	μ_{Fe_I}	1.44	1.60	1.88	2.39	2.55
	$\mu_{Fe_{I-1}}$	2.26	2.28	2.06	2.01	1.98
	μ_{Fe_C}	1.81	2.01	2.04	1.94	1.81

As can be seen in figure 1 the site energies of Mo and Tc lie at higher energies than those of Fe. The hybridization is then stronger for the spin-down bands and its effect is to increase the density of states of the 4d transition metal at lower energies, also increasing the spin-down band occupation, leading to antiferromagnetic ordering. This can also be seen in the densities of states plotted in figures 2(a) and 2(b). The situation is quite different for Rh; in this case the hybridization is almost the same for both spin bands and the polarization of Fe drives the ferromagnetic polarization of Rh. The case of Pd is more complicated, and this simple explanation is not enough. Since the d bands are almost full the magnetic coupling is determined by the shape of the density of states at E_F rather than the position of the band centre. In figure 2(e) it can be seen that the two highest peaks of the d band of Pd are split oppositely to those of Fe, but both of them are well below the Fermi energy. The small hybridization of the minority bands increases the density of states of Pd at energies

just above the Fermi level leading to a larger occupation of the spin-up band. The case of Ru is a special one for as its site energies fall in between the minority bands of Fe it is not clear whether hybridization will turn the down bands of Ru to lower or higher energies. Actually some of the d bands of Ru couple ferromagnetically to Fe while others couple antiferromagnetically.

Applying this simple picture to 4d transition metals grown on Co we would expect the transition from ferromagnetic to antiferromagnetic coupling to occur between Rh and Ru and the magnetic moments to be lower than when grown on Fe. The main reason for this is that the d-band centres of Co lie at lower energies than those of Fe and the exchange splitting is smaller.

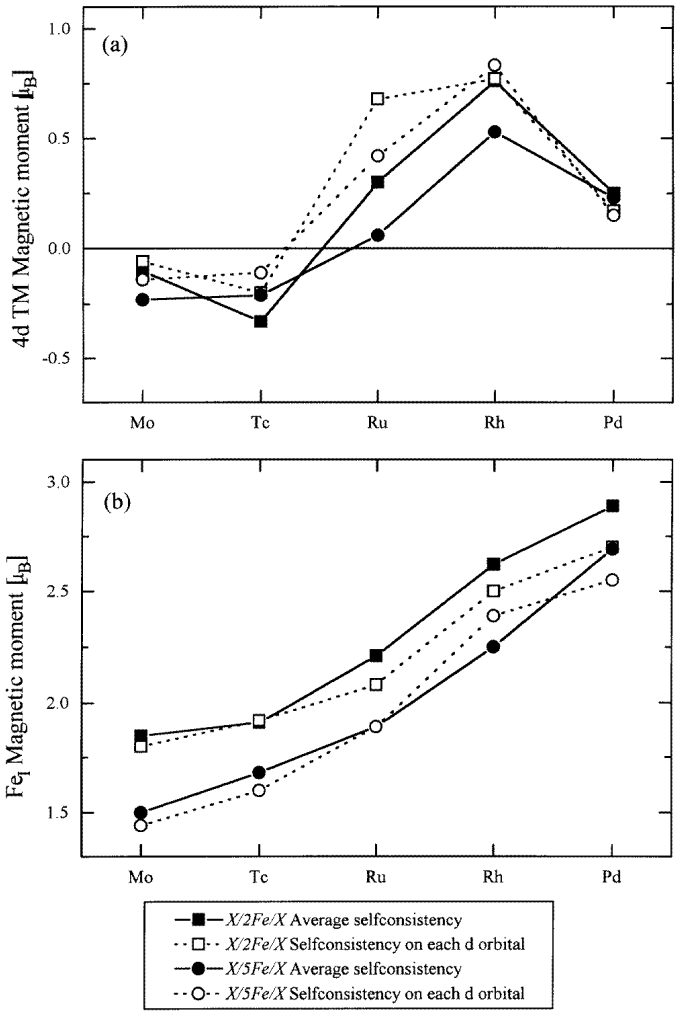

Figure 3. The magnetic moment per atom of the (a) 4d transition metal and (b) interfacial Fe as a function of the 4d transition metal.

From the results of tables 1 and 2 one would expect that those obtained by performing selfconsistency on each d orbital for the X/5Fe/X slabs should be the more accurate as five

layers of Fe should represent better the growth of monolayers on bulk Fe and no average magnetization is assumed. This is confirmed by the good agreement obtained for Ru, Rh and Pd monolayers on Fe when compared with FLAPW results [2, 3]. When the densities of states plotted in figure 2 are compared with those of references [6, 7, 8] it is clear that the bandwidth is larger. This indicates that while 4d transition metal monolayers grown on Ag or Au acquire a magnetic moment due mostly to low dimensionality, in the case of Fe the polarization is due to the hybridization of the d band of the 4d transition metal with the d band of iron. Figure 3(a) shows the magnetic moment of the 4d transition metal as a function of d-band filling. It resembles the one obtained for 3d transition metal monolayers on Fe(001) [17] but shifted one element to the right and with smaller magnetic moments. This effect is the same as that reported by Blügel when going from 3d to 4d and from 4d to 5d transition metal monolayers grown on Ag(001) [8]. It can also be seen that Ru presents the larger variations between the different calculations. Small changes in the Ru site energies, of the order of 0.2 eV, strongly affect the results obtained for the Ru magnetization, even giving antiferromagnetic ordering. This kind of instability was not obtained in any other 4d transition metal for which small changes in the initial site energies only slightly modified the results. This critical magnetic behaviour of Ru has already been found in other calculations [16]. In figure 3(b) we see that the magnetic moment of interfacial iron grows continuously when going from Mo to Pd; the same effect is seen in 3d transition metals grown on Fe when going from V to Cu [17].

Table 3. Magnetizations (μ_B) of the different d orbitals of the 4d transition metal in the X/5Fe/X slabs (X = Mo, Tc, Ru, Rh, Pd) and the expectation values of the spin dipole operator ($\hbar$).

Orbital	Mo	Tc	Ru	Rh	Pd
d_{xy}	0.01	0.00	0.00	0.06	0.03
$d_{zx} = d_{yz}$	−0.06	−0.06	−0.02	0.10	0.04
$d_{x^2-y^2}$	−0.01	0.00	−0.04	−0.05	0.06
$d_{3z^2-r^2}$	−0.01	0.03	0.51	0.65	0.02
$7\langle T_z\rangle$	−0.14	−0.06	1.06	1.48	−0.06

Table 3 shows the selfconsistent magnetic moments per orbital in the X/5Fe/X slabs (the same trend appears in the X/2Fe/X slabs but is not shown). It can be seen that antiferromagnetism is mainly due to the d_{zx} and d_{yz} orbitals, while the ferromagnetic coupling comes mostly from the $d_{3z^2-r^2}$ orbital, except in the case of Pd where this orbital is almost fully occupied. Also shown in table 3 is the *z*-component of the d-electron expectation value of the intra-atomic magnetic dipole operator $\boldsymbol{T} = \boldsymbol{S} - 3\hat{\boldsymbol{r}}\,(\hat{\boldsymbol{r}} \cdot \boldsymbol{S})$. This reflects the anisotropy of the electron spin density and according to the recently derived dichroism sum rules [18, 19, 21] $7\langle T_z\rangle$ could be measured by x-ray magnetic circular dichroism. We see that the positive and large $\langle T_z\rangle$ obtained for Rh and Ru is due to the strong spin polarization of the $d_{3z^2-r^2}$ orbital whereas for Mo, Tc and Pd $\langle T_z\rangle$ is small and has the opposite sign. Through the spin–orbit interaction the spin moment will tend to align with the orbital moment $\langle \overline{L}\rangle$, giving rise to the magnetic anisotropy. Both $\langle T_z\rangle$ and $\langle L_z\rangle$ reflect anisotropies, the former in the spin density and the latter in the charge density. Although the relationship between $\langle T_z\rangle$ and the magnetic anisotropy is still a matter of discussion [20, 21, 22], our results indicate a different magnetic anisotropy for Ru and Rh to that for Mo, Tc and Pd.

4. Conclusions

We have proved that 4d transition metal monolayers grown on bcc-Fe acquire a magnetic moment mainly due to hybridization with Fe bands. This magnetic coupling can be parallel or antiparallel to Fe depending on the relative positions of the corresponding site energies. This can be summarized as follows.

(1) When the bulk paramagnetic site energies of the overlayer lie at higher energies than those of the ferromagnetic substrate, antiferromagnetic coupling is obtained.

(2) When the bulk paramagnetic site energies of the overlayer lie in between the majority and minority bands of the ferromagnetic substrate, ferromagnetic coupling results.

(3) When the bulk paramagnetic site energies of the overlayer lie at nearly the same or lower energies than the majority bands of the substrate, the magnetic coupling is determined by the shape of the density of states at E_F.

Calculations which perform selfconsistency on each d orbital separately have shown that antiferromagnetism is associated with d_{yz}- and d_{zx}-orbital polarization while ferromagnetism shows mainly $d_{3z^2-y^2}$ and $d_{x^2-y^2}$ character. The results for $7\langle T_z\rangle$ show that magnetic anisotropy of Ru and Rh is expected to be different from that of Mo, Tc and Pd.

It is interesting to point out that a thin slab like X/2Fe/X is sufficient for a qualitative analysis, although the results obtained for X/5Fe/X with selfconsistency for each d orbital show a better agreement with FLAPW results.

Acknowledgments

We thank Dr M A Khan for useful discussions and Dr G Fabricius for the tight-binding codes. We acknowledge the Consejo Nacional de Investigaciones Científicas y Técnicas and Fundación Antorchas for partial support of this project.

References

[1] Totland K, Fuchs P, Grölbi J C and Landolt M 1993 *Phys. Rev. Lett.* **70** 2487
[2] Rader O, Carbone C, Clemens W, Vescovo W, Blügel S, Eberhardt W and Gudat W 1992 *Phys. Rev.* B **45** 13 823
[3] Kachel T, Gudat W, Carbone C, Vescovo E, Blügel E, Altkemper U and Eberhardt W 1992 *Phys. Rev.* B **46** 12 888
[4] Pfandzelter R, Steierl G and Rau C 1995 *Phys. Rev. Lett.* **74** 3467
[5] Zhu M J, Bylander D M and Klenman L 1991 *Phys. Rev.* B **43** 4007
[6] Blügel S 1995 *Phys. Rev.* B **51** 2025
[7] Blügel S 1992 *Solid State Commun.* **84** 621
[8] Blügel S 1992 *Phys. Rev. Lett.* **68** 851
[9] Fabricius G, Llois A M, Weissmann M and Khan M A 1994 *Phys. Rev.* B **49** 2121
[10] Fabricius G, Llois A M and Weissmann M 1994 *J. Phys.: Condens. Matter* **6** 5017
[11] Fabricius G, Llois A M, Weissmann M, Khan M A and Dreyssé H 1995 *Surf. Sci.* **331** 1377
[12] Andersen O K, Jepsen O and Glötzel D 1984 *Highlights of Condensed Matter Theory* (Amsterdam: North-Holland)
[13] Andersen O K and Jepsen O 1984 *Phys. Rev. Lett.* **53** 2571
[14] Bandyopadhyay T and Sarma D D 1989 *Phys. Rev.* B **39** 3517
[15] Cunningham S L 1974 *Phys. Rev.* B **10** 4988
[16] Eriksson O, Albers R C and Boring A M 1991 *Phys. Rev. Lett.* **66** 1350
[17] Mirbt S, Eriksson O, Johansson B and Skriver H L 1995 *Phys. Rev.* B **52** 15 070
[18] Thole B T, Carra P, Sette F and van der Laan G 1992 *Phys. Rev. Lett.* **68** 1943
[19] Carra P, Thole B T, Altarelli M and Wang X 1993 *Phys. Rev. Lett.* **70** 694

[20] Weller D *et al* 1995 *Phys. Rev. Lett.* **75** 3752
[21] Sthör J and König H 1995 *Phys. Rev. Lett.* **75** 3748
[22] Wu R and Freeman A J 1994 *Phys. Rev. Lett.* **73** 1994